

S.Ya. Pukas¹, L.A. Zinko¹, N.V. German¹, R.E. Gladyshevskii¹,
I.V. Koval², L.G. Bodrova², H.M. Kramar², S.Yu. Marynenko²

Influence of the Nano-WC Content and Sintering Temperature on the Phase Composition of Hard Alloys in the System TiC–WC–VC–NiCr

¹Ivan Franko National University of Lviv, Lviv, Ukraine, svitlana.pukas@lnu.edu.ua
²Ternopil Ivan Puluj National Technical University, Ternopil, Ukraine, vr@tu.edu.te.ua

The effect of the WC content and the sintering temperature, as the main technological factor, on the phase composition of TiC–*x*WC–5VC–18NiCr alloys was investigated by X-ray phase analysis. It was established that the main phases in the investigated alloys were the NaCl-type quaternary (Ti,V,W)C phase and a solid solution of Cr in Ni. Depending on the size of the WC particles used for the preparation, the metal binder could be described by the formula Ni_{0.75}Cr_{0.25} (for nano WC) or Ni_{0.5}Cr_{0.5} (for fine-sized WC). In alloys prepared with fine-sized WC, elementary Cr and traces of the Cr₃C₂ and Cr₂₃C₆ were also found. With increasing content of nano-sized WC and sintering temperature the solubility of W in (Ti,V)C increased. No W₂C phase was detected under the conditions of the investigation.

Keywords: hard alloy, nano WC, fine-sized WC, X-ray powder diffraction, phase composition.

Received 14 July 2020; Accepted 15 September 2020.

Introduction

Improvements of the quality of hard alloys, and enhancements of their physical, mechanical and operational properties, may be achieved by different methods [1-5], including optimization of the chemical composition [6, 7], in particular by adding alloying additives in the nano-dispersed state [8, 9]. Alloying of carbides or metal binders by nanocarbitides or nanometals increases the strength, hardness, and wear resistance of the alloys [10, 11]. It is known [12-14] that one of the reasons for specific properties of nanomaterials is the increase of the volume fraction of interface boundaries with decreasing size of the grains or crystals. There is, however, no unique opinion regarding the nature of the process.

Tungsten carbide is an efficient additive for hard alloys based on titanium carbide, since it increases the mechanical and operational properties [15]. For alloys on a polycarbide base, for example, TiC–VC–NbC, nano-sized powder additives have an even stronger positive

effect [16, 17].

The influence of additives of nano-sized WC on the properties of the hard alloy WC–8Co was investigated in [18]. The authors consider that one of the reasons for the increased hardness of the alloys with nano-sized WC additives was the formation of a cubic modification of W₂C in the process of sintering the alloys and its effect on the mechanical properties. According to their data the content of W₂C phase was 5 - 8 wt.% after sintering.

W₂C was also claimed to have a positive effect on the properties, in particular increase of the hardness and abrasive stability, of alloys in the system W₂C–(Co,Ni) [19], as well as on the operational properties of WC/M-composites and coatings [20, 21].

According to the phase diagram of the tungsten-carbon system, the W₂C phase exists only at high temperature; it forms above 1250°C and has a broad homogeneity range (from 25 to 33 at.% C near the melting point) [22, 23]. Several polymorphic modifications of W₂C tungsten carbide are known and identified as rhombohedral, orthorhombic, hexagonal, and trigonal, in addition to the cubic modification

mentioned above. According to *ab initio* calculations (full-potential linearized augmented planewave FLAPW with generalized gradient correction GGA), only the rhombohedral and orthorhombic modifications were found to be thermodynamically stable [24]. Kublii and Velikanova [23] identified two modifications in the phase diagram, formed above and below approx. 1850°C, respectively, both with hexagonal structures. The distribution of the carbon atoms is generally considered to be disordered at high temperature and (partly) ordered at lower temperatures.

The crystal and electronic structures of the phases in the W–C system, methods and conditions for obtaining W₂C (including nano-sized) are analysed in [25]. However, some discrepancies regarding the generation and identification of the polymorphic modifications of W₂C remain.

The aim of this work was to study the influence of nano and fine-sized WC and sintering temperature, the latter being the main technological factor, on the phase composition of TiC–*x*WC–5VC–18NiCr alloys and the possibility of formation of a W₂C phase in this heterogeneous system during sintering.

I. Materials and methods

TiC–*x*WC–5VC–18NiCr alloys containing 5, 10, and 15 wt.% nano WC (commercial, grain size 150 - 200 nm) and 5 wt.% fine-sized WC (commercial, grain size 1 - 2 μm) were prepared. The alloys were sintered at a temperature of 1400°C in a vacuum of 1.33×10⁻² Pa, holding time 20 min. To determine the effect of the sintering temperature on the phase composition, alloys with the highest content of nano WC (15 wt.%) were

sintered at 1300, 1350, 1400, and 1450°C. The initial composition of the investigated alloys and the sintering temperatures are summarized in Table 1.

Phase analysis of synthesized alloys was performed based on X-ray powder diffraction data collected on a DRON-4.0M diffractometer (Fe K α radiation) [26]. The data collection was carried out according to the Bragg-Brentano scheme: a flat sample and the counter rotating in a horizontal plane around the vertical axis of the goniometer. Studies of individual alloys were also performed with Co K α radiation. Pearson's Crystal Data Database was used to identify the phases [27]. The structural parameters were refined using the Rietveld method [28], which is based on a full-profile analysis, using the DBWS program [29]. The crystallographic parameters of the compounds in the W–C system [27, 30] are summarized in Table 2 and were used for comparison.

II. Results and discussion

The main phases in all the samples alloyed by nano WC, regardless of the sintering temperature, were (Ti,V,W)C and (Ni,Cr), crystallizing with the cubic structure types NaCl (Pearson symbol *cF8*, space group *Fm-3m*) and Cu (Pearson symbol *cF4*, space group *Fm-3m*), respectively. The results of the X-ray phase analysis, the content of phases (ω), the unit-cell parameter of the phases (*a*), as well as the reliability factors (R_B – Bragg factor for the phase (Ti,V,W)C, R_p – profile factor for the diffraction pattern) are presented in Table 3.

The quaternary (Ti,V,W)C phase is a solid solution of V and W in the binary compound TiC. It is known

Table 1

Alloy No.	Nominal composition, wt.%					Sintering temperature, °C
	TiC	VC	WC	Ni	Cr	
1	72	5	5 (fine-sized)	13.5	4.5	1400
2	72	5	5 (nano)	13.5	4.5	1400
3	67	5	10 (nano)	13.5	4.5	1400
4	62	5	15 (nano)	13.5	4.5	1400
5	62	5	15 (nano)	13.5	4.5	1300
6	62	5	15 (nano)	13.5	4.5	1350
7	62	5	15 (nano)	13.5	4.5	1450
8	72	5	5 (nano)	13.5	4.5	1300
9	72	5	5 (nano)	13.5	4.5	1350

Table 2

Compound	Structure type	Pearson symbol	Space group	Unit-cell parameters		
				<i>a</i> , nm	<i>b</i> , nm	<i>c</i> , nm
W ₃ C _{0.375}	Cr ₃ Si	<i>cP8</i>	<i>Pm-3n</i>	0.5041	–	–
WC _{0.5} ht2	NiAs	<i>hP4</i>	<i>P6₃/mmc</i>	0.2996	–	0.4724
W ₂ C ht1	W ₂ C	<i>hP12</i>	<i>P-31m</i>	0.5162	–	0.4739
W ₂ C trig	CdI ₂	<i>hP3</i>	<i>P-3m1</i>	0.29948	–	0.47262
W ₂ C orth	Fe ₂ N _{0.94}	<i>oP12</i>	<i>Pbcn</i>	0.4721	0.6030	0.5180
WC _{0.8} ht	NaCl	<i>cF8</i>	<i>Fm-3m</i>	0.4215	–	–
WC	WC	<i>hP2</i>	<i>P-6m2</i>	0.2901	–	0.2830

Table 3

Results (weight fractions, unit-cell parameters, reliability factors) of the X-ray phase analysis of the samples alloyed by nano WC

Alloy No.	(Ti,V,W)C				Ni _{0.75} Cr _{0.25}		R _p
	ω, wt.%	a, nm	Ti/W	R _B	ω, wt.%	a, nm	
2	95(5)	0.43148(7)	0.999(6)/ 0.001(6)	0.0614	5(5)	0.35807(9)	0.0511
3	85(4)	0.42985(6)	0.998(7)/ 0.002(7)	0.0692	15(3)	0.35639(5)	0.0388
4	85(4)	0.42978(6)	0.978(7)/ 0.022(7)	0.0377	15(2)	0.35632(5)	0.0420
5	88(5)	0.43063(7)	0.983(8)/ 0.017(8)	0.0461	12(4)	0.35738(6)	0.0481
6	90(3)	0.43047(5)	0.981(6)/ 0.019(6)	0.0655	10(2)	0.35791(4)	0.0339
7	85(3)	0.43030(4)	0.971(6)/ 0.029(6)	0.0404	15(2)	0.35700(3)	0.0317

Table 4

Results (weight fractions, unit-cell parameters, reliability factors) of the X-ray phase analysis of the alloy with 5 wt.% fine-sized WC

Alloy No.	(Ti,V,W)C				Ni _{0.5} Cr _{0.5}		Cr		R _p
	ω, wt.%	a, nm	Ti/W	R _B	ω, wt.%	a, nm	ω, wt.%	a, nm	
1	87(3)	0.43083(5)	1.0/0.0	0.0572	6(4)	0.36012(6)	7(4)	0.28892(5)	0.0405

[22] that titanium and vanadium carbides in the TiC–VC system form continuous rows of solid solutions (TiC_{0.95}–VC_{0.88}); in the system TiC–WC at 1500°C there is a limited solid solution (TiC_{0.95}–Ti_{0.55}W_{0.45}C). For the quaternary (Ti,V,W)C phase only the (Ti,V)/W ratio was determined (see Table 3), since the scattering abilities of the Ti and V atoms are approximately the same.

The (Ni,Cr) phase is a solid solution of Cr in Ni, the composition of which was fixed at a Ni to Cr ratio of 3:1 and described by the formula Ni_{0.75}Cr_{0.25}, in accordance with the ratio of the metal binder components in the samples.

For an alloy containing 5 wt.% nano WC, the solubility of W in the (Ti,V)C phase is 0.88 at.%; by increasing the content of nano WC to 15 wt.% the solubility of W increases to 1.32 at.% [31]. This increase of the solubility is well reflected by the change of the unit-cell parameter: in the first case, the cell parameter is $a = 0.43148(7)$ nm, and on further substitution of W atoms for Ti atoms the unit-cell parameter decreases to $a = 0.42985(6)$ nm (alloy with 10 wt.% nano WC) and $a = 0.42978(6)$ nm (alloy with 15 wt.% nano WC), which is consistent with the atomic radii of Ti ($r = 0.147$ nm) and W ($r = 0.139$ nm).

The X-ray diffraction pattern of the sample alloyed with fine-sized WC contained reflections corresponding to the phases (Ti,V,W)C and (Ni,Cr), but also body-centred Cr (structure type W, Pearson symbol *cI2*, space group *Im-3m*), and traces of Cr₃C₂ and Cr₂₃C₆. It should be noted that the composition of the phase (Ni,Cr) in this sample was described by the formula Ni_{0.5}Cr_{0.5}, based on the unit-cell parameter ($a = 0.36012(6)$ nm), which was significantly different from the unit-cell parameter of the phase assigned the composition Ni_{0.75}Cr_{0.25} ($a = 0.35807(9) - 0.35632(5)$ nm).

The phase composition of the alloys with 5 wt.%

fine-sized WC is presented in Table 4. The unit-cell parameter of the (Ti,V,W)C phase in this alloy ($a = 0.43083(5)$ nm) is slightly smaller than the parameter in the nano WC alloy ($a = 0.43148(7)$ nm), which may indicate a larger amount of W in (Ti,V)C.

Observed, calculated and difference X-ray powder diffraction patterns of the alloys with different WC contents are shown on Fig. 1, whereas Fig. 2 shows patterns of the alloys with 15 wt.% nano-sized WC submitted to different sintering temperatures. The solubility of W in the (Ti,V)C phase is illustrated on Fig. 3.

As can be seen from Table 3, in the alloy with 5 wt.% nano WC the content of the Ni_{0.75}Cr_{0.25} phase is 2 - 3 times lower than in the alloys with 10 and 15 wt.% nano WC. For the samples with a content of 15 wt.% nano WC, prepared at different sintering temperatures, an increase of the solubility of W in the TiC phase (from 0.85 to 1.5 at.% W) was observed on increasing the sintering temperature from 1300 to 1450°C.

Increasing the content of nano WC, or increasing the sintering temperature, leads to an increase of the amount of W dissolved in the (Ti,V)C phase and a decrease of the unit-cell parameter of the quaternary (Ti,V,W)C phase from $a = 0.43063(7)$ nm to $a = 0.42978(6)$ nm (see Table 3), up to the sintering temperature 1400°C. For the sintering temperature 1450°C, an increase of the unit-cell parameter to $a = 0.43030(4)$ nm was observed.

For the highest sintering temperatures (1400°C and 1450°C), the maximum content of the Ni_{0.75}Cr_{0.25} phase was observed in alloys containing 10 and 15 wt.% nano WC. The intensity of the reflections belonging to the Ni_{0.75}Cr_{0.25} phase on the X-ray powder diffraction patterns is consistent with the intensity of the reflections on the powder pattern calculated for this phase (Fig. 4),

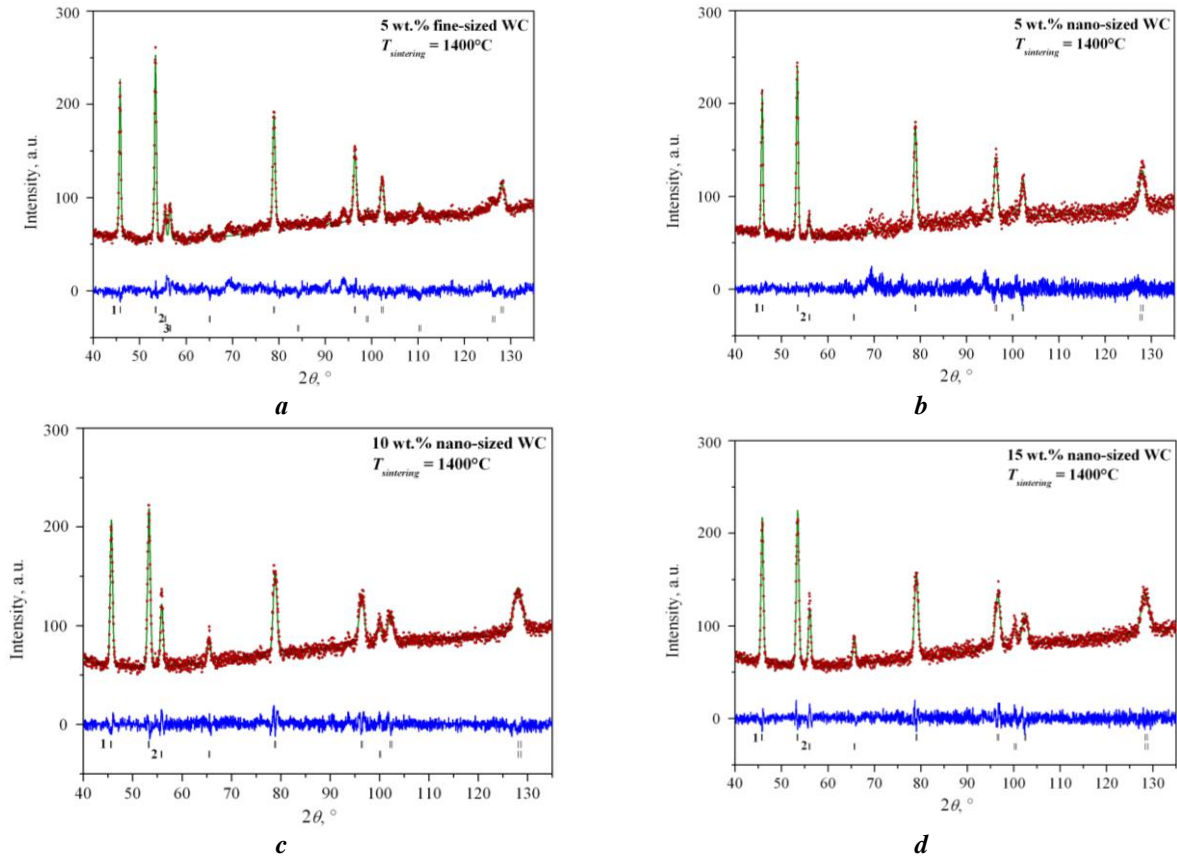


Fig. 1. Observed (dots), calculated (line) and difference (bottom) X-ray powder diffraction patterns of the alloys with 5 wt.% fine-sized WC (a), 5 wt.% (b), 10 wt.% (c), and 15 wt.% (d) nano WC; vertical bars indicate the positions of the reflections of the phases (Ti,V,W)C (1), Ni_{0.75}Cr_{0.25} (or Ni_{0.5}Cr_{0.5} in the case of the alloy with 5 wt.% fine-sized WC) (2) and Cr (3).

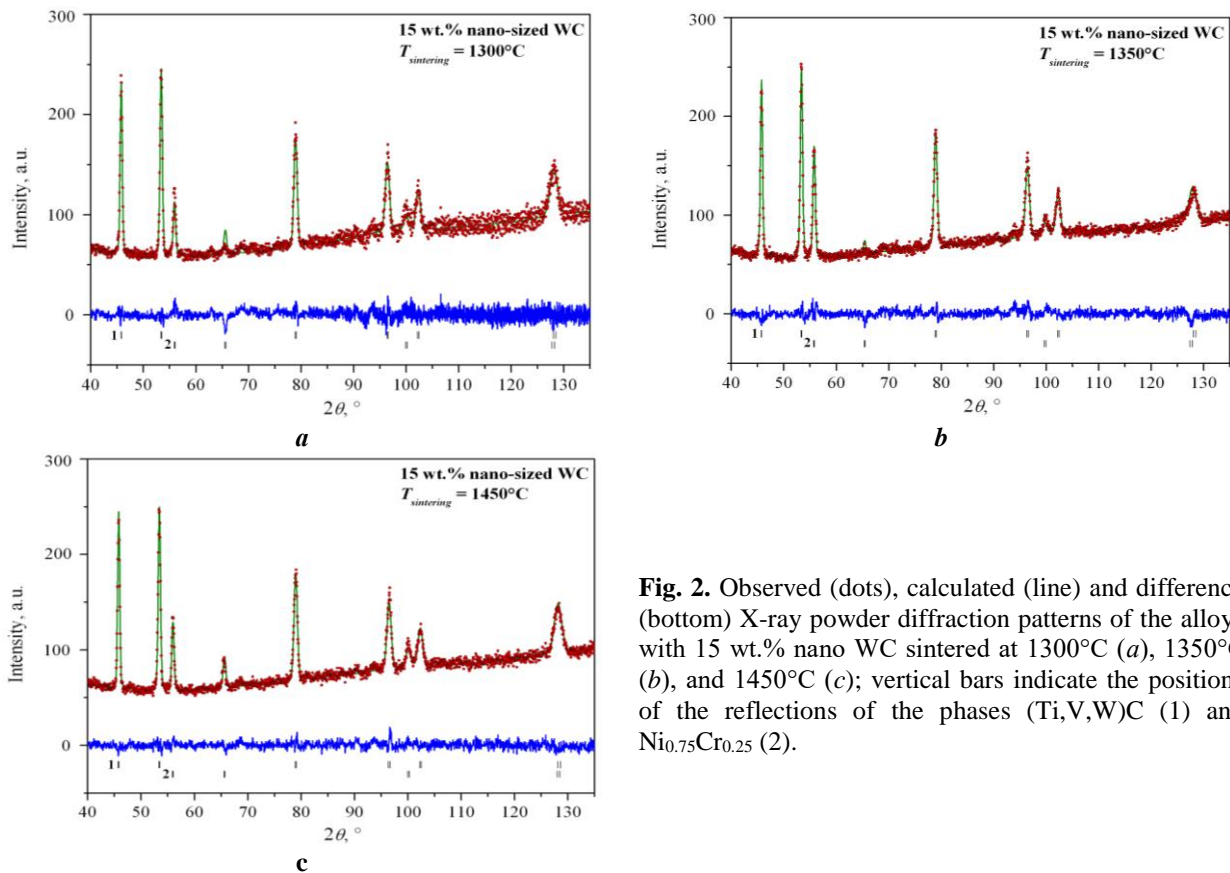


Fig. 2. Observed (dots), calculated (line) and difference (bottom) X-ray powder diffraction patterns of the alloys with 15 wt.% nano WC sintered at 1300°C (a), 1350°C (b), and 1450°C (c); vertical bars indicate the positions of the reflections of the phases (Ti,V,W)C (1) and Ni_{0.75}Cr_{0.25} (2).

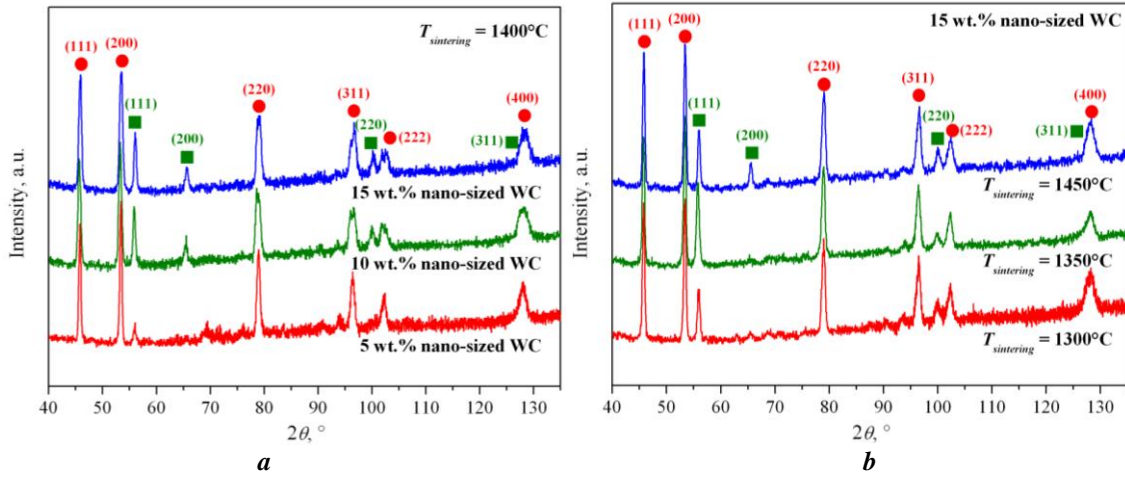


Fig. 3. Observed X-ray powder diffraction patterns of the alloys with 5, 10, and 15 wt.% nano WC sintered at 1400°C (a) and with 15 wt.% of nano WC sintered at 1300, 1350, and 1450°C (b) (● – positions of the reflections of the phase $(\text{Ti,V,W})\text{C}$, ■ – positions of the reflections of the phase $\text{Ni}_{0.75}\text{Cr}_{0.25}$).

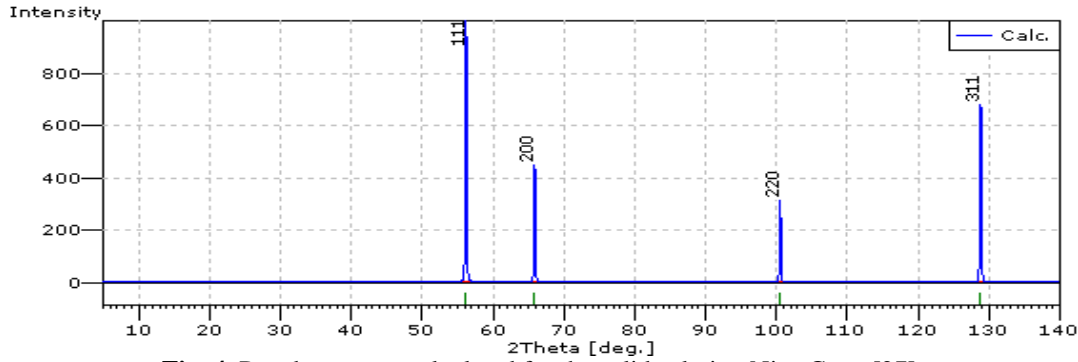


Fig. 4. Powder pattern calculated for the solid solution $\text{Ni}_{0.75}\text{Cr}_{0.25}$ [27].

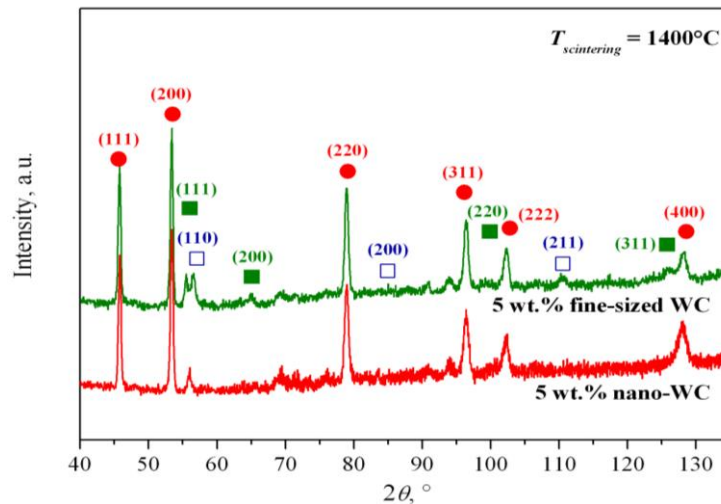


Fig. 5. Observed X-ray powder diffraction patterns of the alloys with 5 wt.% fine-sized and nano WC sintered at 1400°C (● – positions of the reflections of the phase $(\text{Ti,V,W})\text{C}$, ■ – positions of the reflections of the phase $\text{Ni}_{0.75}\text{Cr}_{0.25}$ (or $\text{Ni}_{0.5}\text{Cr}_{0.5}$), □ – positions of the reflections of elementary Cr).

whereas the intensity of the reflection with the indexes (200) of the phase $\text{Ni}_{0.75}\text{Cr}_{0.25}$ for alloys, prepared at the sintering temperatures 1350 and 1400°C , is very weak, which may be due to the texture of these samples.

The X-ray powder diffraction patterns of the alloys with 5 wt.% nano- and fine-sized WC are shown in Fig. 5. The difference between these powder patterns is the displacement of the reflections of the (Ni,Cr) phase due to the different Ni/Cr ratios and, consequently, unit-cell

parameters, as well as the presence of elementary Cr in the sample alloyed by fine-sized WC.

The influence of the sintering temperature on the phase composition was confirmed by an additional investigation of the sample alloyed by 5 wt.% nano WC with $\text{Co K}\alpha$ -radiation (Fig. 6).

Consequently, the X-ray phase analysis identified the following main phases: in alloys with nano WC, regardless of the initial WC content and sintering

temperature, the main phases were (Ti,V,W)C and $\text{Ni}_{0.75}\text{Cr}_{0.25}$, and in the alloy alloyed with fine-sized WC, – (Ti,V,W)C, $\text{Ni}_{0.5}\text{Cr}_{0.5}$, elementary Cr, and traces of Cr_3C_2 and Cr_{23}C_6 . With the alloying of fine-sized WC part of Cr is not incorporated into Ni, but forms chromium carbides or remains in the free state.

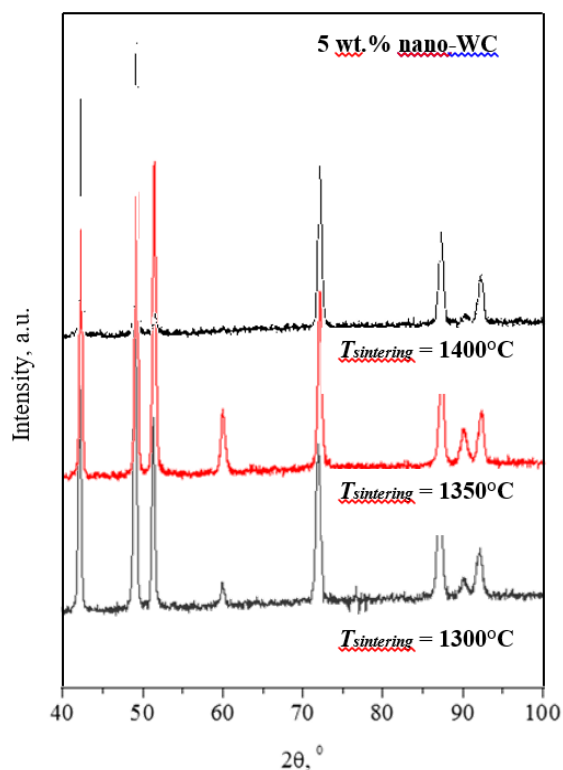


Fig. 6. Observed X-ray powder diffraction patterns of the alloys with 5 wt.% nano WC prepared at the sintering temperatures 1300, 1350, and 1450°C.

The W_2C phase was not detected in any of the investigated alloys, regardless of the grain size of the WC additive, its content or the sintering temperature.

Conclusions

The phase composition of $\text{TiC-xWC-5VC-18NiCr}$

alloys prepared from nano and fine-sized particles of WC was studied. The main phases present in the alloys prepared from nano WC were (Ti,V,W)C and $\text{Ni}_{0.75}\text{Cr}_{0.25}$ at all the investigated sintering temperatures, whereas the alloys prepared with fine-sized WC contained (Ti,V,W)C, $\text{Ni}_{0.5}\text{Cr}_{0.5}$, elementary Cr, and traces of Cr_3C_2 and Cr_{23}C_6 . With increasing nano WC content, the amount of W in the (Ti,V)C phase increased and the unit-cell parameter of the resulting quaternary (Ti,V,W)C phase decreased from $a = 0.43148(7)$ nm to $a = 0.42978(6)$ nm.

A similar tendency, *i.e.* an increase of the solubility of W in (Ti,V)C and a decrease of the unit-cell parameter $a = 0.43063(7)$ - $0.42978(6)$ nm was observed when the sintering temperature was increased (up to 1400°C). A W_2C phase was not detected in any of the investigated samples, regardless of the sintering temperature.

In the samples alloyed by nano WC, the solid solution of Cr in Ni was conveniently described by the composition of $\text{Ni}_{0.75}\text{Cr}_{0.25}$, whereas in the sample alloyed by fine-sized WC it was better described by the composition $\text{Ni}_{0.5}\text{Cr}_{0.5}$.

Pukas S.Ya. - PhD (in Chemical Sciences), Associate Professor at the Department of Inorganic Chemistry;
Zinko L.A. – Master in Chemistry, PhD student at the Department of Inorganic Chemistry;
German N.V. – Head of the laboratory at the Department of Inorganic Chemistry;
Gladyshevskii R.E. – Professor, Corresponding Member of the NAS of Ukraine, DSc (in Chemical Sciences), Director of the Department of Inorganic Chemistry, Vice-Rector for Science and Research;
Koval I.V. – PhD (in Technical Sciences), Associate Professor at the Department of Structural Mechanics;
Bodrova L.G. – PhD (in Technical Sciences), Professor at the Department of Structural Mechanics;
Kramar H.M. – PhD (in Technical Sciences), Associate Professor at the Department of Structural Mechanics;
Marynenko S.Yu. – PhD (in Technical Sciences), Associate Professor at the Department of Technology and Equipment of Welding.

- [1] A. Laptiev, Z. Pakiel, O. Tolochyn, T. Brynk, J. Alloys Compd. 687, 135 (2016) (doi: 10.1016/j.jallcom.2016.05.343).
- [2] Z. Fu, J.H. Kong, S.R. Gajjala, R. Koc, J. Alloys Compd. 751, 316 (2018) (doi: 10.1016/j.jallcom.2018.04.124).
- [3] S. Yi, H. Yin, J. Zheng, D.F. Khan, X. Qu, Comput. Mater. Sci. 79, 417 (2013) (doi: 10.1016/j.commatsci.2013.06.031).
- [4] Y. Xu, Y. Zhang, S. Z. Hao, O. Perroud, C. Dong, Appl. Surf. Sci. 279, 137 (2013) (doi: 10.1016/j.apsusc.2013.04.053).
- [5] J. Pötschke, T. Gestrich, V. Richter, Int. J. Refract. Met. Hard Mater. 72, 117 (2018) (doi: 10.1016/j.jirmhm.2017.12.016).
- [6] D.V. Suetin, N.I. Medvedeva, J. Alloys Compd. 681, 508 (2016) (doi: 10.1016/j.jallcom.2016.04.279).
- [7] I. Konyashin, L.I. Klyachko, Int. J. Refract. Met. Hard Mater. 49, 9 (2015) (doi: 10.1016/j.jirmhm.2014.08.011).
- [8] F.F. Mammadov, IFAC-PapersOnLine 51(30), 641 (2018) (doi: 10.1016/j.ifacol.2018.11.231).
- [9] J. Sun, J. Zhao, Z. Li, X. Ni, A. Li, Ceram. Int. 43(2), 2686 (2017) (doi: 10.1016/j.ceramint.2016.11.086).
- [10] L. Bodrova, G. Kramar, I. Koval, V. Sushynskiy, S. Marynenko, V. Bukhta, Euromat 2011 (European Congress on Advanced Materials and Processes) (Montpellier 2 Univ., Montpellier, France, 2011), p. 1408.

- [11] V.I. Sushynskiy, H.M. Kramar, Ye.O. Isaiev, Specificity of Polycarbide Sintering Based on Hard Alloys with Fine- and Nano-sized Binder (Publishing Center of "Polytechnica" of Igor Sikorsky KPI, Kyiv, Ukraine, 2011).
- [12] S. Naboychenko, N.A. Yefimov, Handbook of Non-Ferrous Metal Powders: Technologies and Applications, Second Edition (O.D. Neikov (Ed.), Elsevier, Amsterdam, 2019).
- [13] N. Alharbi, K. Benyounis, L. Looney, J. Stokes, Synthesis and Properties of Nanostructured Cermet Coatings, In: Reference Module in Materials Science and Materials Engineering, (Elsevier, Amsterdam, 2018) (doi: 10.1016/B978-0-12-803581-8.10179-1).
- [14] A. Rajabi, M.J. Ghazali, Ceram. Int. 43(16), 14233 (2017) (doi: 10.1016/j.ceramint.2017.07.171).
- [15] J. Xiong, Z. Guo, B. Shen, D. Cao, Materials & Design 28(5), 1689 (2007) (doi: 10.1016/j.matdes.2006.03.005).
- [16] H.M. Kramar, L.H. Bodrova, M.M. Prokopiv, S.Yu. Marynenko, 18 Plansee seminar 2013 – International Conference on Refractory Metals and Hard Materials (Plansee SE, Reutte, Austria, 2013), p. 146.
- [17] O.V. Mul, I.V. Koval, L.G. Bodrova, H.M. Kramar, Euro PM2015 Proceedings: Hard Materials - Processing, 4 p. (2015).
- [18] Y. Sun, W. Su, H. Yang, J. Ruan, Ceram. Int. 41(10), 14482 (2015) (doi: 10.1016/j.ceramint.2015.07.086).
- [19] A. Klimpel, L.A. Dobrzański, A. Lisiecki, D. Janicki, J. Mater. Process. Technol. 164-165, 1068 (2005) (doi: 10.1016/j.jmatprotec.2005.02.198).
- [20] T. Li, Q. Li, J.Y.H. Fuh, P.C. Yu, C.C. Wu, Mater. Sci. & Eng. A 430(1-2), 113 (2006) (doi: 10.1016/j.msea.2006.05.118).
- [21] M.F. Morks, Y. Gao, N.F. Fahim, F.U. Yingqing, Mater. Lett. 60(8), 1049 (2006) (doi: 10.1016/j.matlet.2005.10.073).
- [22] H. Okamoto, Desk Handbook: Phase Diagrams for Binary Alloys (American Society for Metals, Materials Park, Ohio, USA, 2000).
- [23] V.Z. Kublii, T.Ya. Velikanova, Powder Metall. Met. Ceram. 43, 630 (2004) (doi: 10.1007/s11106-005-0032-3).
- [24] A.I. Gusev, A.S. Kurlov, JETP Lett. (2007) (doi: 10/1134/s0021364007010079).
- [25] F.I. Chaplygin, Tungsten carbides (state diagram, crystal and electronic structure of structural phases of the W–C system) (2012) (www.kamet.com.ua/attachments/article/74/kv_1_2_1.pdf).
- [26] R.E. Gladyshevskii, Methods to Determine Crystal Structures. Textbook (Publishing Centre of Ivan Franko National University of Lviv, Lviv, Ukraine, 2015).
- [27] P. Villars, K. Cenzual (Eds.), Pearson's Crystal Data. Crystal Structure Database for Inorganic Compounds, Release 2015/16 (ASM International, Materials Park, Ohio, USA, 2015).
- [28] R.A. Young (Ed.), The Rietveld Method (Oxford University Press, Oxford, United Kingdom, 1995).
- [29] R.A. Young, A. Sakthivel, T.S. Moss, C.O. Paiva-Santos, J. Appl. Crystallogr. 28, 366 (1995).
- [30] P. Villars, K. Cenzual, J.L.C. Daams, F. Hulliger, H. Okamoto, K. Osaki, A. Prince, S. Iwata, Pauling File. Inorganic Materials Database and Design System. Binaries Edition (Crystal Impact (Distributor), Bonn, Germany, 2001).
- [31] L. Bodrova, H. Kramar, Ya. Kovalchuk, S. Marynenko, I. Koval, Sci. J. Riga Techn. Univ. 57, 35 (2018).

С.Я. Пукас¹, Л.А. Зінько¹, Н.В. Герман¹, Р.Є. Гладішевський¹,
І.В. Коваль², Л.Г. Бодрова², Г.М. Крамар², С.Ю. Мариненко²

Вплив вмісту нано-WC і температури спікання на фазовий склад твердих сплавів системи TiC–WC–VC–NiCr

¹Львівський національний університет імені Івана Франка, Львів, Україна, svitlana.pukas@lnu.edu.ua
²Тернопільський національний технічний університет імені Івана Пулюя, Тернопіль, Україна, vr@tu.edu.te.ua

Методом рентгенівського фазового аналізу досліджено вплив вмісту WC і температури спікання як основного технологічного чинника, на фазовий склад сплавів TiC–xWC–5VC–18NiCr. Встановлено, що основними фазами у досліджуваних сплавах є тетрарна фаза (Ti,V,W)C і твердий розчин Cr в Ni зі структурами типу NaCl. Залежно від розміру частинок легуючого WC, металева зв'язка описується формулою Ni_{0,75}Cr_{0,25} (для нано WC) або Ni_{0,5}Cr_{0,5} (для дрібнодисперсного WC). У сплавах, легованих дрібнодисперсним WC, виявлено також елементарний Cr і сліди фаз Cr₃C₂ та Cr₂₃C₆. При збільшенні вмісту нано-розмірного WC і підвищенні температури спікання розчинність W в (Ti,V)C зростає. Фази W₂C, при умовах дослідження, не виявлено.

Ключові слова: твердий сплав, нано WC, рентгенівська порошкова дифракція, фазовий склад.